Supporting Information

Small molecular acceptors with a ladder-like core for high-performance organic solar cells with low non-radiative energy losses

Yunzhi Wang,[a] Zhongwei Liu,[b] Xinyue Cui,[a] Chu Wang,[a] Hao Lu,[a] Yahui Liu,*[a] Zhuping Fei,[b] Zaifei Ma,[c] and Zhishan Bo*[a]

[a] Key Laboratory of Energy Conversion and Storage Materials, Key Laboratory of Theoretical and Computational Photochemistry, Ministry of Education, College of Chemistry, Beijing Normal University, Beijing 100875, P. R. China

E-mail: lyh1991a@163.com, zsbo@bnu.edu.cn

[b] Institute of Molecular Plus, Tianjin Key Laboratory of Molecular Optoelectronic Science, Tianjin University, Tianjin, 300072, P. R. China

[c] Center for Advanced Low-Dimension Materials, State Key Laboratory for Modification of Chemical Fibers and Polymer Materials, College of Materials Science and Engineering, Donghua University, Shanghai 201620, P. R. China

1.1 Material and Instruments

Unless otherwise noted, all chemicals were purchased from Aldrich or Acros and used without further purification. The catalyst precursor $Pd(PPh_3)_4$ was prepared according to the literature and stored in a Schlenk tube under nitrogen atmosphere. Unless otherwise noted, all reactions were performed under an atmosphere of nitrogen and monitored by thin layer chromatography (TLC) on silica gel. Column chromatography was carried out on silica gel (200-300 mesh). ^1H and ^{13}C NMR spectra were recorded on a Bruker AV 500 spectrometer or a Bruker AV 600 spectrometer. UV-visible absorption spectra were obtained on a PerkinElmer UV-vis spectrometer model Lambda 750. Elemental analyses were performed on a Flash EA 1112 analyzer. Thermal gravimetric analysis (TGA) was performed on TA2100 , under a nitrogen atmosphere at a heating rate of 10 ℃/min to record TGA curves. Atomic force microscopy (AFM) measurements were performed under ambient conditions using a Digital Instrument Multimode Nanoscope IIIA operating in the tapping mode. The thickness of the blend films was determined by a Dektak 6 M surface profilometer. The powder X-ray diffraction (XRD) patterns were collected using a PANalytical X'Pert PRO MPD diffractometer with Cu KR radiation. The electrochemical behavior of the accepters was investigated using cyclic voltammetry (CHI 630A Electrochemical Analyzer) with a standard three-electrode electrochemical cell in a 0.1 M Bu_4NPF_6 solution in CH_3CN at room temperature

under an atmosphere of nitrogen with a scanning rate of 0.1 V/S. A Pt plate working electrode, a Pt wire counter electrode, and an $Ag/AgNO_3$ (0.01 M in CH_3CN) reference electrode were used. The experiments were calibrated with the standard ferrocene/ferrocenium (F_c) redox system and assumption that the energy level of F_c is 4.8 eV below vacuum.

1.2 Solar Cell Fabrication and Characterization

OSCs were fabricated with the device configuration of ITO/ZnO/active layer (100 nm)/MoO_3 (85 Å)/Ag (100 nm). The conductivity of ITO is 20 Ω. A mixture of **PBDB-T** and acceptor molecule (**BT-IC4F**, **BT2F-IC4F** or **BTOR-IC4F**) in 1,2-dichlorobenzene (DCB) was stirred at 110 ℃ at least two hours to ensure sufficient dissolution and then the blend solution was spin-coated onto ZnO layer to form active layer. On one substrate five cells with an effective area of 0.04 cm^2 for each were fabricated. Current-voltage characteristics were recorded using an Enli Technology Ltd., Taiwan (SS-F53A) under an AM 1.5G AAA class solar simulator with an intensity of 100 mW cm^{-2} as the white light source and the intensity was calibrated with a standard single crystal Si photovoltaic cell. The temperature while measuring the *J-V* curves was approximately 25 ℃. The EQE measurements of OSCs were performed by the solar cell spectral response measurement system QE-R3011 (Enli Technology Ltd., Taiwan), which was calibrated by monocrystalline silicon solar cell in advance.

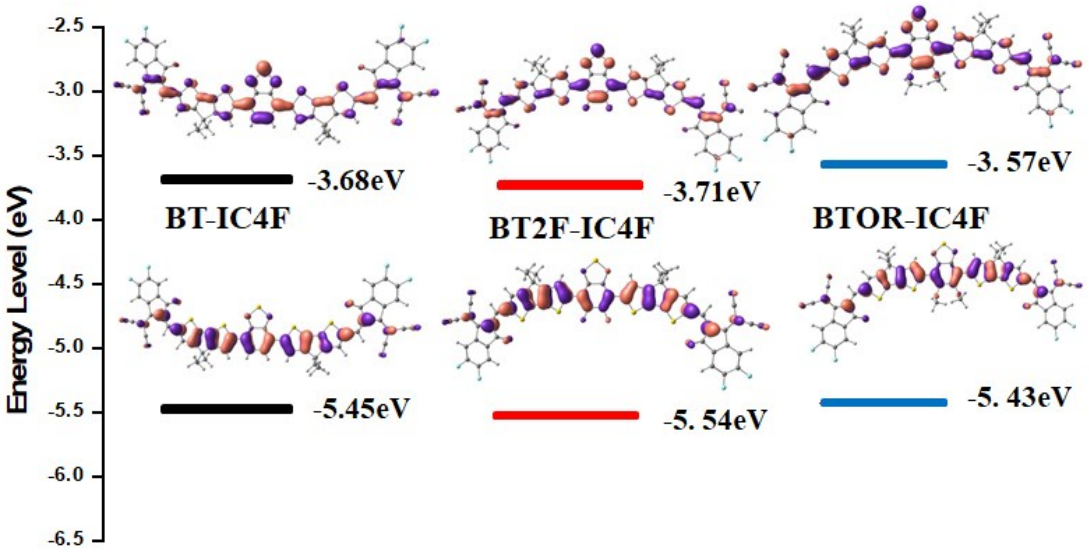

Figure S1. Energy levels of simplified **BT-IC4F**, **BT2F-IC4F** and **BTOR-IC4F** determined via DFT calculations.

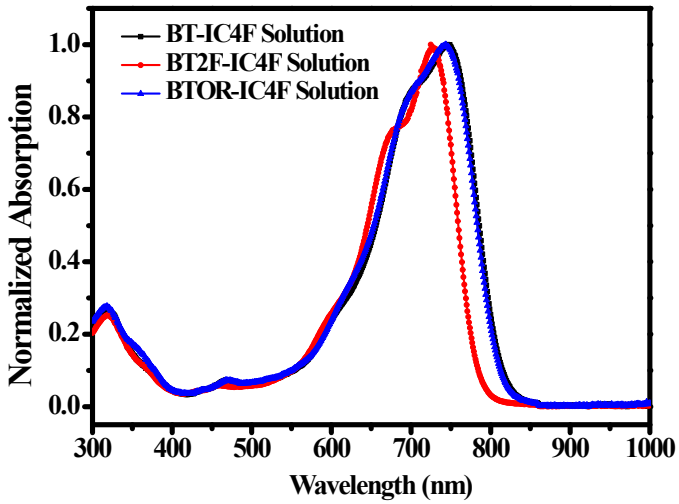

Figure S2. Normalized absorption spectra of **BT-IC4F**, **BT2F-IC4F** and **BTOR-IC4F** in chloroform solutions.

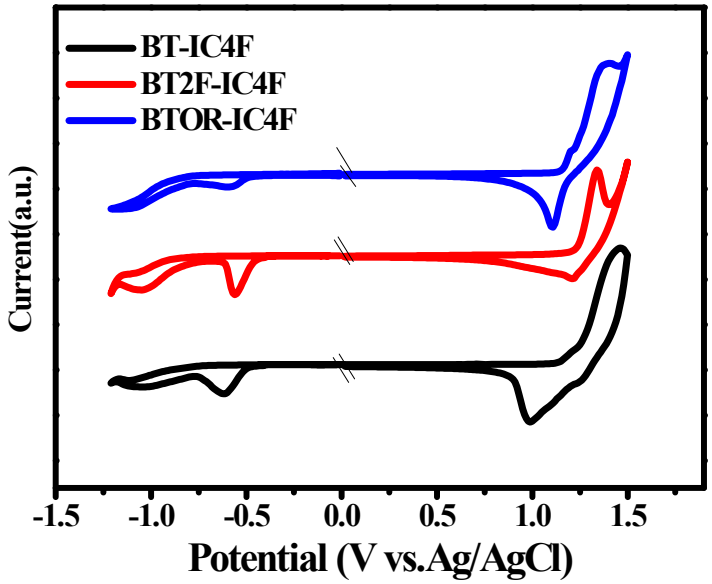

Figure S3. CV curves of **BT-IC4F**, **BT2F-IC4F** and **BTOR-IC4F**.

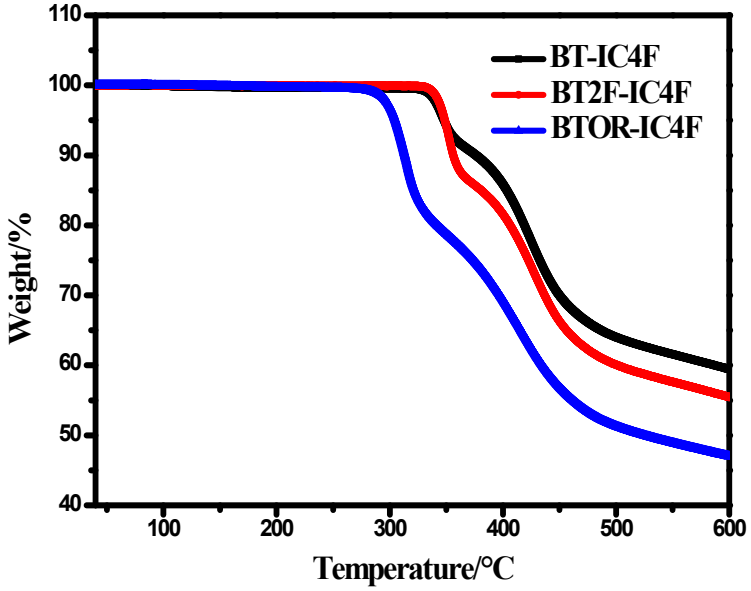

Figure S4. TGA plot of **BT-IC4F**, **BT2F-IC4F** and **BTOR-IC4F**.

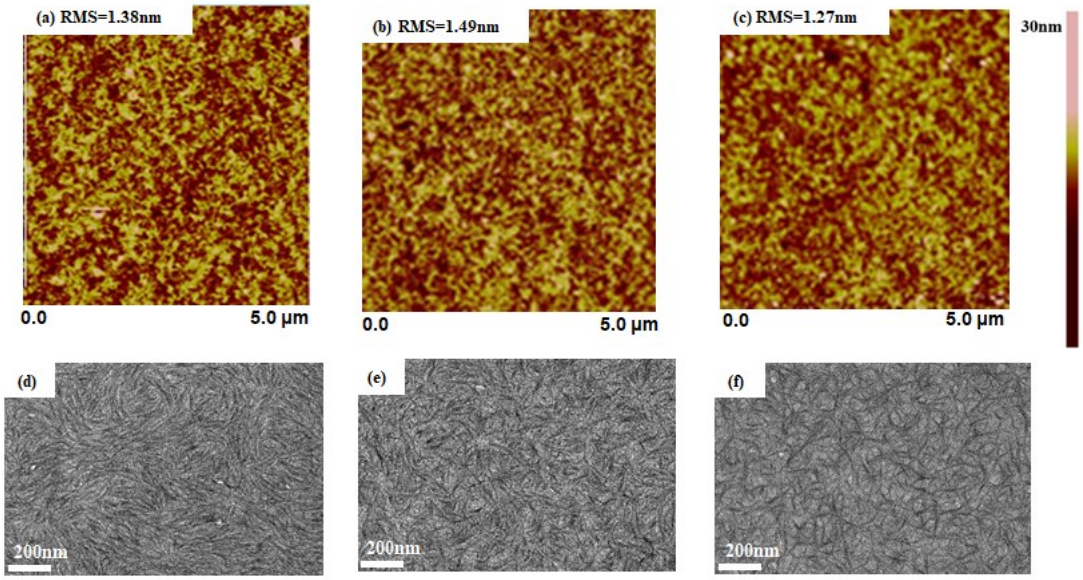

Figure S5. AFM and TEM images for as-cast blend films based on **BT-IC4F** a,d); **BT2F-IC4F** b,e); **BTOR-IC4F** c,f).

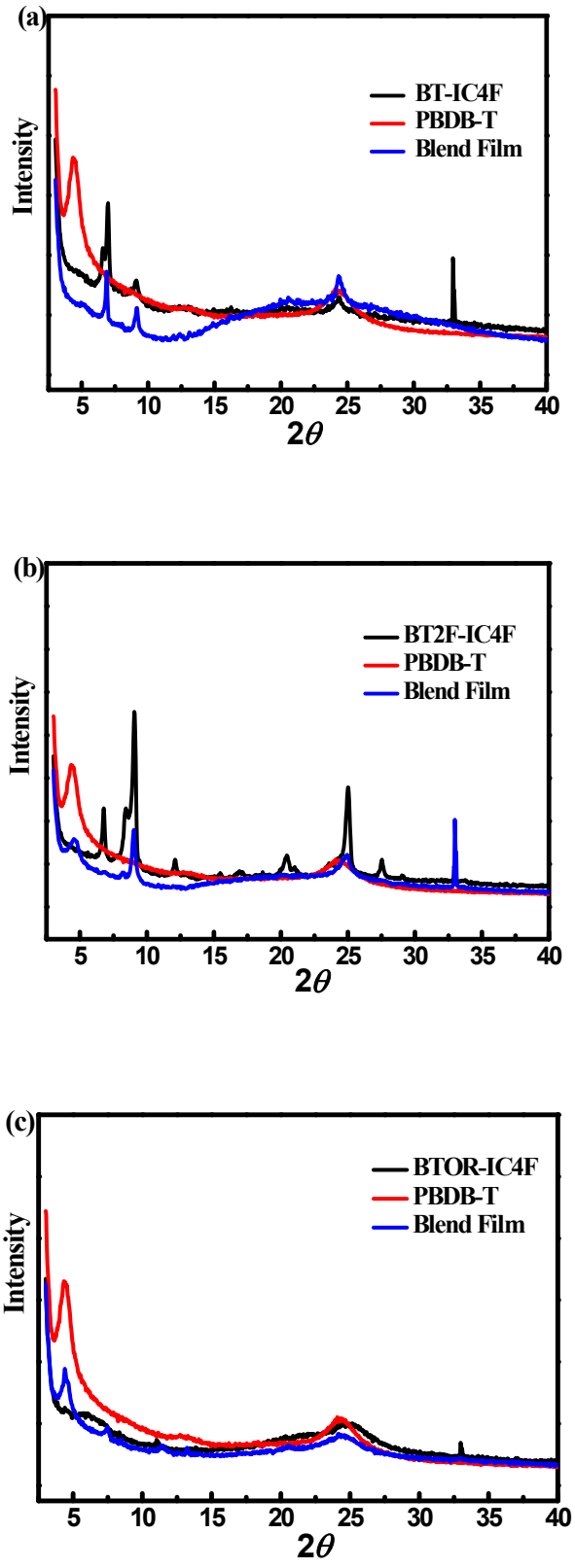

Figure S6. XRD curves of **BT-IC4F** (a), **BT2F-IC4F** (b), **BTOR-IC4F** (c), PBDB-T and the blend films.

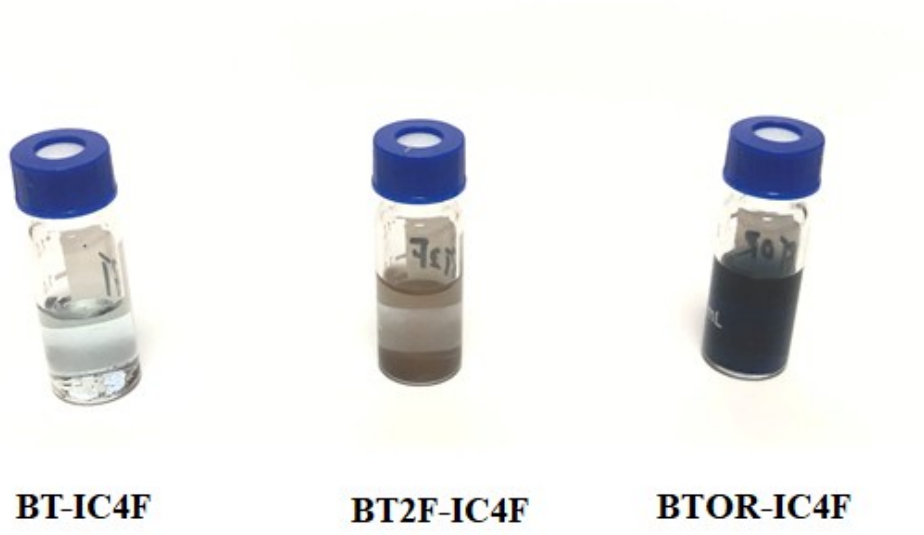

Figure S7. Photographs illustrating the different solubilities of **BT-IC4F**, **BT2F-IC4F** and **BTOR-IC4F** in n-hexane solutions with the same solid content of 0.5 mg/mL.

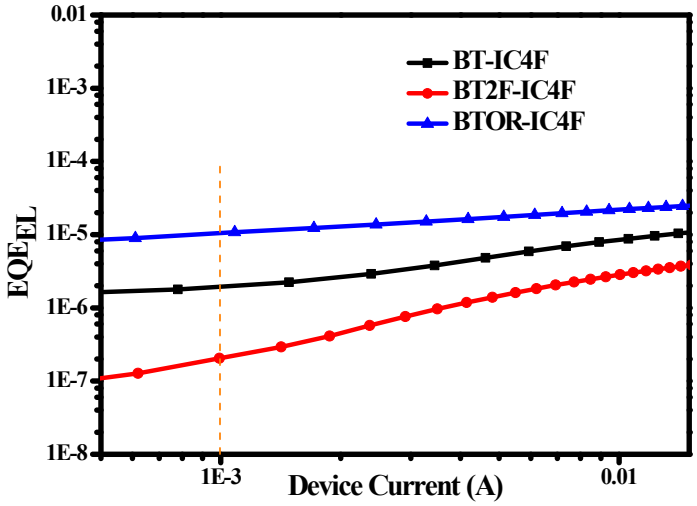

Figure S8. EQE_{EL} of the solar cells based on different acceptors.

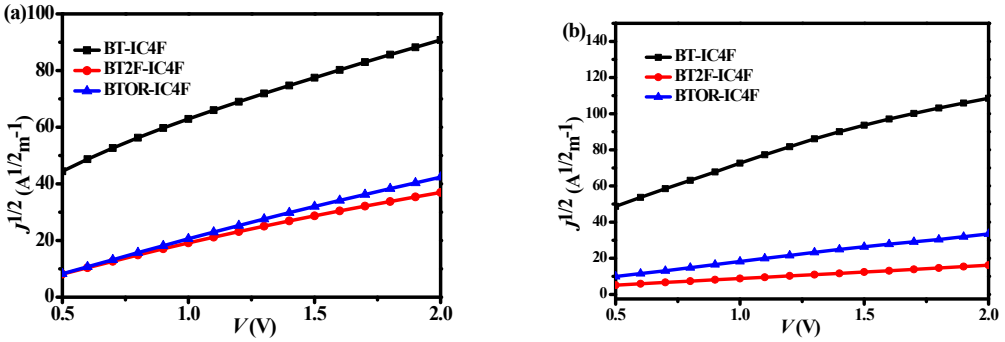

Figure S9. $J^{1/2}$–V curves for determining hole (a) and electron (b) mobilities of **BT-IC4F**, **BT2F-IC4F** and **BTOR-IC4F** based devices.

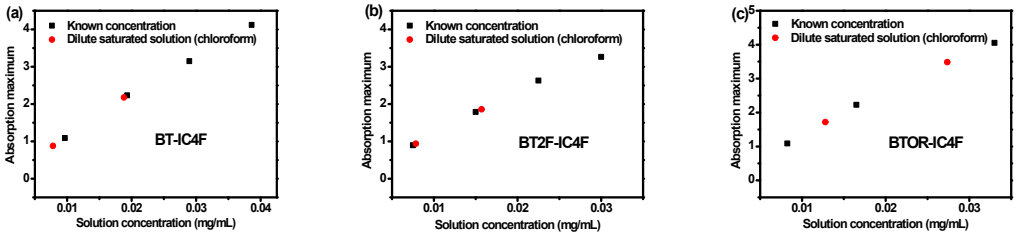

Figure S10. Plot of absorption maximum vs. solution concentration for a) **BT-IC4F**, b) **BT2F-IC4F**, c) **BTOR-IC4F**. The solubilities of **BT-IC4F**, **BT2F-IC4F**, **BTOR-IC4F** are 141, 118, 192 mg/mL as derived from concentration and absorption data.

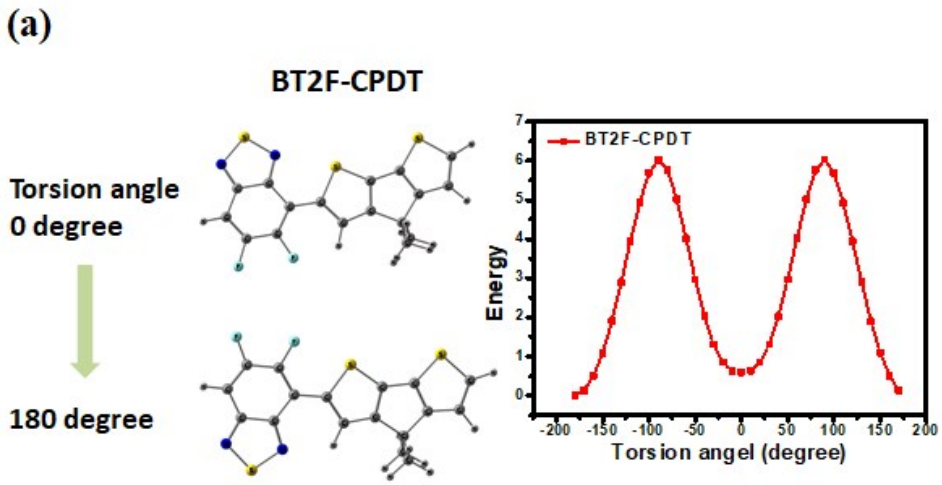

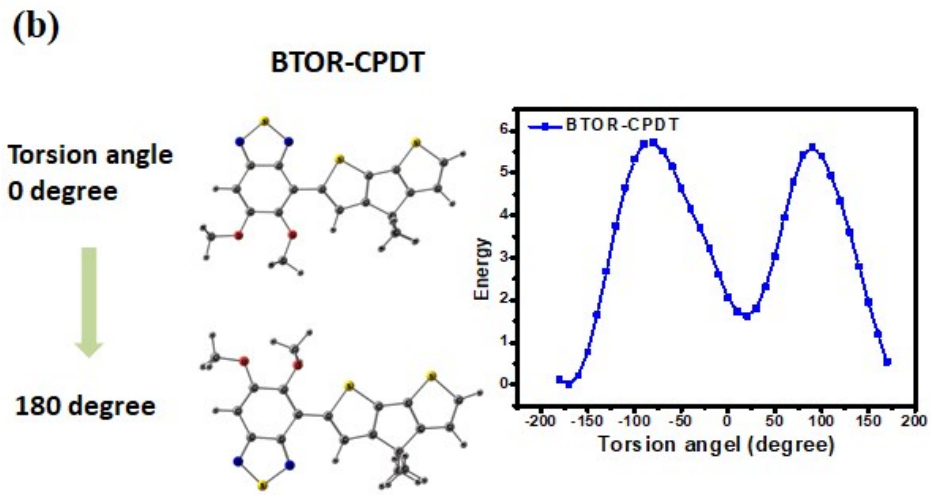

Figure S11. Potential energy surface scans of a) BT2F-CPDT rotamer and b) BTOR-CPDT rotamer.

Table S1. Photovoltaic performance of the solar cells based on PBDB-T:**BT-IC4F**, PBDB-T:**BT2F-IC4F** and PBDB-T:**BTOR-IC4F** with different D:A ratio.

Active layer	D：A ratio(w/w)	V_{OC}(V)	J_{SC}(mA cm^{-2})	FF	PCE(%)
	1:0.8	0.71	11.06	41.9	3.29
PBDB-T	1:1	0.71	15.37	59.7	6.55
/BT-IC4F	1:1.2	0.71	19.13	57.6	7.85
	1:1.4	0.70	15.60	51.8	5.67
PBDB-T	1:1	0.71	12.32	62.9	5.52
/BT2F-IC4F	1:1.2	0.71	16.82	58.3	7.04
	1:1.4	0.72	17.19	54.7	6.79
PBDB-T	1:1	0.82	18.03	63.7	9.46
/BTOR-IC4F	1：1.2	0.81	19.70	63.8	10.18

	1:1.4	0.82	19.30	63.1	9.97

Table S2. Photovoltaic performance of the solar cells based on PBDB-T:**BT-IC4F**, PBDB-T:**BT2F-IC4F** and PBDB-T:**BTOR-IC4F** processed by DCB and varied amount of 1-chloronaphthalene (CN).

Active layer	CN(vol%)	V_{OC}(V)	J_{SC}(mA cm^{-2})	FF	PCE(%)
PBDB-T	0.1%	0.70	16.74	58.6	6.91
/**BT-**	0.2%	0.71	17.39	61.8	7.66
IC4F=1:1.2	0.5%	0.72	14.90	66.0	7.13
	1.0%	0.68	16.32	61.3	6.90
PBDB-T	0.1%	0.70	15.35	60.7	6.60
/**BT2F-IC4F**	0.2%	0.71	16.63	57.9	6.86
=1:1.2	0.5%	0.69	16.72	67.4	7.87
	0.75%	0.70	14.95	68.2	7.14
PBDB-T	0.1%	0.81	18.91	63.7	9.86
/**BTOR-IC4F**	0.2%	0.81	18.19	68.4	10.15
=1:1.2	0.5%	0.81	19.36	67.6	10.66
	0.75	0.80	18.83	66.5	10.14
	1.0%	0.80	18.23	64.9	9.53

Table S3. Different annealing temperature of devices based on **BT-IC4F**, **BT2F-IC4F** and **BTOR-IC4F** with D:A ratio of 1:1.2 and annealing time of 10 min.

Active layer	Annealing Temperature	V_{OC}(V)	J_{SC}(mA cm^{-2})	FF	PCE(%)

PBDB-T	90	0.69	19.23	66.0	8.79
/BT-IC4F	110	0.69	18.01	68.1	8.46
	130	0.69	21.40	66.4	9.83
	150	0.68	18.63	66.3	8.48
PBDB-T	80	0.68	17.11	66.4	7.80
/BT2F-IC4F	90	0.67	19.43	64.7	8.45
	100	0.67	17.44	67.1	7.95
	110	0.68	17.01	67.9	7.88
	120	0.67	17.98	63.5	7.68
PBDB-T	80	0.80	18.18	71.9	10.50
/BTOR-IC4F	90	0.80	20.02	70.5	11.36
	100	0.80	18.89	70.5	10.70
	110	0.80	18.58	71.8	10.70
	120	0.79	17.03	67.0	9.09

Table S4. Different annealing time of devices based on **BT-IC4F** with D:A ratio of 1:1.2 and annealing temperature of 130℃.

Active layer	Annealing time(min)	V_{OC}(V)	J_{SC}(mA cm^{-2})	FF	PCE(%)
PBDB-T	5	0.68	19.69	67.1	9.09
/BT-IC4F	10	0.69	21.40	66.4	9.83
	15	0.68	20.65	67.5	9.59
	20	0.68	19.65	68.92	9.29

Table S5. Different annealing time of devices based on **BTOR-IC4F** with D:A ratio of 1:1.2 and annealing temperature of 90℃.

Active layer	Annealing time(min)	V_{OC}(V)	J_{SC}(mA cm^{-2})	FF	PCE(%)
PBDB-T	5	0.80	19.37	71.7	11.15
/**BTOR-IC4F**	10	0.80	20.57	69.6	11.48
	15	0.79	19.40	71.2	10.97

Table S6. Hole and electron mobilities of devices with **BT-IC4F**, **BT2F-IC4F** and **BTOR-IC4F**.

Acceptors	μ_h (cm^2 V^{-1} s^{-1})	μ_e (cm^2 V^{-1} s^{-1})	μ_h /μ_e	Thickness (nm)
BT-IC4F	1.63×10^{-4}	2.92×10^{-4}	0.55	81
BT2F-IC4F	8.99×10^{-5}	1.30×10^{-5}	6.92	90
BTOR-IC4F	1.34×10^{-4}	7.17×10^{-5}	1.85	94

1.3 Experimental Section

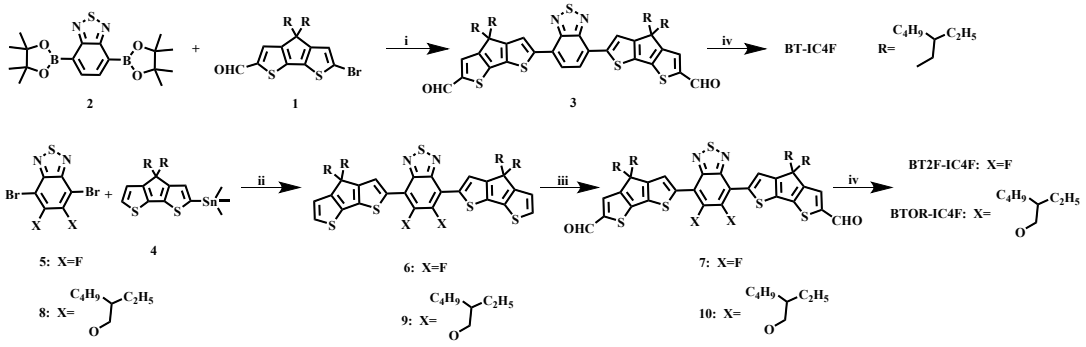

Synthesis of BT-IC4F

Synthesis of 3

The original material 2 was purchased and 1 was produced according to the reported method[10.1016/j.dyepig.2013.08.016]. A mixture of 1 (200 mg, 0.38 mmol), 2 (55 mg, 0.14 mmol), $NaHCO_3$ (117 mg, 1.4mmol), THF (15 mL) and H_2O (2 mL) was carefully degassed before and after $Pd(PPh_3)_4$ added. After refluxed under N_2 atmosphere for 8 hours, water and ethyl acetate were added, the organic layer was separated. The water phase was washed with ethyl acetate for three times. The combined organic layer was dried with anhydrous $MgSO_4$ and filtrated, the organic solvent was moved under reduced pressure. The residue was purified by chromatography on silica gel column eluting with DCM/petrol ether (3:1) to give product 3 (120 mg, 88%) as an orange solid.

^{1}H NMR (600 MHz, $CDCl_3$) δ: 9.85 (s, 2H), 8.12 (d, *J* = 6.3Hz, 2H), 7.90 (s, 2H), 7.60 (t, *J* = 3.5Hz, 2H), 2.02 (m, 8H), 1.59 (s, 4H), 1.08-0.86 (m, 36H), 0.77-0.55 (m, 20H).

^{13}C NMR (150 MHz, $CDCl_3$) δ:182.55, 162.81, 158.30, 152.45, 147.69, 143.80, 143.64, 137.77, 130.69, 126.39, 125.15, 122.94, 54.35, 43.21, 35.46, 34.48, 34.22, 28.68, 28.59, 27.68, 27.43, 22.83, 14.14, 14.01, 10.82, 10.71.

Synthesis of **BT-IC4F**

A mixture of 3 (107 mg, 0.11 mmol), 2-(5,6-difluoro-3-oxo-2,3-dihydro-1*H*-inden-1-ylidene)malononitrile (127mg, 0.55 mmol), and $CHCl_3$ (30 mL) was carefully degassed before the addition of 0.5 mL pyridine. After being stirred at room temperature overnight, the solvent was removed under reduced atmosphere. The residue was purified by chromatography on silica gel eluting with DCM/petrol ether (3:1, v/v) to give **BT-IC4F** (98 mg) as a dark red solid in a yield of 63%.

^{1}H NMR (500 MHz, $CDCl_3$) δ: 8.91 (s, 2H), 8.53 (t, *J* = 10.0Hz, *J* = 6.4Hz, 2H), 7.71 (d, *J* = 1.9Hz, 4H), 7.66 (t, *J* = 7.5Hz, 4H), 7.36 (d, *J* = 1.6Hz, 2H), 2.06-1.94 (m, 8H), 1.04-0.92 (m, 32H), 0.78-0.72 (m, 16H), 0.68-0.62 (m, 12H).

^{13}C NMR (125 MHz, $CDCl_3$) δ: 186.14, 166.25, 159.99, 158.44, 155.30, 153.22, 152.28, 147.40, 139.41, 138.56, 138.18, 136.49, 134.48, 126.61, 125.68, 123.40, 119.66, 114.98, 114.73, 112.44, 68.16, 54.21, 43.23, 35.55, 34.19, 28.49, 27.44, 22.80, 14.06, 10.65.

MS (MALDI-TOF): m/z 1418.1 (M^+).

Synthesis of BTOR-IC4F

Synthesis of 9

Step1: A solution of 4,4-di(2-ethylhexyl)-4H-cyclopenta[2,1-b:3,4-b]dithiophene (600 mg, 1.5 mmol) in THF (20 ml) was cooled to -78 °C in an acetone/dry ice bath. n-Butyllithium in n-hexane (1.6 M, 1.1mL) was added slowly. After 2 h, a solution of trimethyltin chloride in THF (1 M, 1.8 mL) was added in one portion at -78 °C, and the mixture was allowed to warm up to room temperature and stirred for another 6 h. Then the mixture was poured into water and the product was extracted with hexane three times. was dried with anhydrous $MgSO_4$ and filtrated. The solvent was removed

via a rotavapor. The crude product was used in subsequent reactions without further purification (Yield, 91%).

Step2: A mixture of 8 (180 mg, 0.35 mmol) and the crude product (600 mg) in toluene was degassed before and after $Pd(PPh_3)_4$ (30 mg) was added. And the mixture was refluxed under N_2 for 8 hours. After the reaction was finished, toluene was removed out with rotary evaporator. The residue was chromatographically purified on silica gel column with DCM/petroleum ether (1:3, v/v) to give 9 as a purple powder in a yield of 70% (284 mg).

^{1}H NMR (600 MHz, $CDCl_3$) δ: 8.49-8.31 (m, 2H), 7.18 (d, *J* = 4.8Hz, 2H), 6.98 (dt, *J* = 5.0Hz, *J* = 2.6Hz, 2H), 4.01 (dt, *J* = 6.6Hz, *J* = 2.9Hz, 4H), 2.13-1.90 (m, 10H), 1.62-1.24 (m, 20H), 1.08-0.81 (m, 40H), 0.79-0.73 (m, 8H), 0.68-0.58 (m,20H).

^{13}C NMR (150 MHz, $CDCl_3$) δ: 158.20, 157.42, 151.82, 151.08, 139.47, 137.26, 133.93, 125.89, 124.76, 122.46, 117.56, 53.59, 43.39, 40.33, 35.15, 34.21, 30.34, 29.02, 28.67, 27.37, 23.67, 23.19, 22.86, 14.10, 11.10, 10.68

Synthesis of 10

A Vilsmeier reagent, which was prepared with $POCl_3$ (0.50 mL) in DMF (8 mL), was added to a solution of 11 (365mg, 0.31 mmol) in 1,2-dichloroethane (40 mL) under the protection of N_2. After refluxing at 80 °C overnight, the mixture was poured into ice water (100 mL), neutralized with aqueous AcONa, and then extracted with dichloromethane (50 ml × 2). The combined organic layer was washed with water and brine, dried over anhydrous $MgSO_4$. After removal of solvent, the crude product was purified by silica gel to obtain 10 in a yield of 73% (283mg).

^{1}H NMR (600 MHz, $CDCl_3$) δ: 9.85 (s, 2H), 8.59-8.42 (m, 2H), 7.60 (t, *J* = 5.0Hz, 2H), 4.03 (d, *J* = 6.8Hz, 4H), 2.14-1.97 (m, 8H), 1.63-1.27 (m, 16H), 1.08-0.87 (m, 36H), 0.80-0.70 (m, 16H), 0.69-0.57 (22H).

^{13}C NMR (150 MHz, $CDCl_3$) δ:182.54, 161.70, 158.30, 152.59, 150.77, 148.20, 143.49, 138.74, 138.41, 130.83, 126.18, 117.89, 78.74, 54.18, 43.34, 40.44, 35.49, 34.46, 34.21, 30.37, 29.05, 28.70, 28.58, 27.59, 27.44, 23.70, 23.22, 22.87, 14.22, 14.15, 11.13, 10.75.

Synthesis of **BTOR-IC4F**

A mixture of 10 (127 mg, 0.12 mmol), 2-(5,6-difluoro-3-oxo-2,3-dihydro-1*H*-inden-1-ylidene)malononitrile (138mg, 0.60 mmol), and $CHCl_3$ (30 mL) was carefully degassed before the addition of 0.5 mL pyridine. After being stirred at room temperature overnight, the solvent was removed under reduced atmosphere. The residue was purified by chromatography on silica gel eluting with DCM/petrol ether (3:1, v/v) to give **BTOR-IC4F** (173 mg) as a dark red solid in a yield of 62%.

^{1}H NMR (500 MHz, $CDCl_3$) δ: 8.93 (s, 2H), 8.67 (m, 2H), 8.53 (dd, *J* = 10.0Hz, *J* = 6.4Hz, 2H), 7.68 (q, *J* = 8.6Hz, *J* = 7.4Hz, 4H), 4.10 (dt, *J* = 5.7Hz, *J* = 2.9Hz, 4H), 2.19-1.99 (m, 8H), 1.70-1.23 (m, 16H), 1.09-0.87 (m, 44H), 0.82-0.60 (m, 30H).

^{13}C NMR (125 MHz, $CDCl_3$) δ: 186.21, 165.34, 160.20, 159.38, 158.55, 155.24, 153.17, 152.97, 150.46, 142.94, 139.26, 138.27, 136.53, 134.44, 126.61, 119.25, 118.21, 114.87, 112.34, 67.80, 54.00, 43.27, 40.41, 35.56, 34.34, 34.02, 30.34, 29.01, 28.49, 27.50, 27.31, 23.73, 23.20, 22.82, 14.10, 11.08, 10.66.

MS (MALDI-TOF): m/z 1674.4 (M^+).

Synthesis of BT2F-IC4F

Synthesis of 6

6 was synthesized in similar way of 9 in a yield of 69%.

^{1}H NMR (600 MHz, $CDCl_3$) δ: 8.18 (t, 2H), 7.23 (d, *J* = 4.8Hz, 2H), 6.99 (dd, *J* = 4.9Hz, *J* = 3.0Hz, 2H), 2.06-1.89 (m, 8H), 1.26 (m, 4H), 1.04-0.84 (m, 36H), 0.77-0.58 (m, 20H).

^{13}C NMR (150 MHz, $CDCl_3$) δ: 159.08, 157.91, 141.49, 136.79, 131.26, 125.99, 125.78, 122.45, 53.76, 43.26, 35.19, 34.19, 29.72, 28.66, 28.53, 27.46, 27.33, 22.78, 14.08, 13.98, 10.76, 10.62.

Synthesis of 7

7 was synthesized in similar way of 10 in a yield of 71%.

^{1}H NMR (600 MHz, $CDCl_3$) δ: 9.87 (s, 2H), 8.26-8.22 (m, 2H), 7.62 (d, *J* = 5.1Hz, 2H), 2.10-1.95 (m, 8H), 1.04-0.86 (m, 36H), 0.74 (dd, *J* = 7.8Hz, *J* = 6.3Hz, 4H), 0.65-0.57 (20H).

^{13}C NMR (150 MHz, $CDCl_3$) δ:182.64, 161.77, 158.86, 148.65, 147.13, 144.27, 140.16, 135.65, 130.64, 125.96, 112.08, 54.29, 43.11, 35.36, 34.42, 34.12, 29.71, 28.60, 28.48, 27.57, 27.30, 22.75, 14.06, 13.95, 10.72, 10.60.

Synthesis of **BT2F-IC4F**

BT2F-IC4F was synthesized in similar way of **BTOR-IC4F** in a yield of 61%.

^{1}H NMR (500 MHz, $CDCl_3$) δ: 8.95 (s, 2H), 8.56 (dd, *J* = 9.9Hz, *J* = 6.4Hz, 2H), 8.37 (t, *J* = 7.6Hz, 2H), 7.72 (t, *J* = 7.5Hz, 4H), 2.21-1.96 (m, 8H), 1.57(s, 4H), 1.12-0.95 (m, 32H), 0.80-0.54 (m, 24H).

^{13}C NMR (125 MHz, $CDCl_3$) δ: 186.07, 164.88, 160.43, 158.43, 157.50, 155.32, 153.29, 148.48, 140.89, 139.74, 139.24, 138.22, 136.52, 134.48, 126.22, 120.16, 114.93, 114.54, 112.54,68.64, 54.21, 43.21, 35.54, 34.36, 34.03, 28.48, 27.55, 27.29, 22.79, 14.03, 10.63.

MS (MALDI-TOF): m/z 1453.1 (M^+).